J/ψ, ψ' and DY production in proton nucleus collisions at 450 GeV incident energy at the NA50 experiment

M.C. Abreu[6,a], B. Alessandro[10], C. Alexa[3], R. Arnaldi[10], M. Atayan[12], C. Baglin[1], A. Baldit[2], M. Bedjidian[11], S. Beolè[10], V. Boldea[3], P. Bordalo[6,b], S.R. Borenstein[9,c], G. Borges[6], A. Bussière[1], L. Capelli[11], J. Castor[2], C. Castanier[2], B. Chaurand[9], B. Cheynis[11], E. Chiavassa[10], C. Cicalò[4], T. Claudino[6], M.P. Comets[8], N. Constans[9], S. Constantinescu[3], P. Cortese[10,d], J. Cruz[6], N. De Marco[10], A. De Falco[4], G. Dellacasa[10,d], A. Devaux[2], S. Dita[3], O. Drapier[11], B. Espagnon[2], J. Fargeix[2], P. Force[2], M. Gallio[10], Y.K. Gavrilov[7], C. Gerschel[8], P. Giubellino[10], M.B. Golubeva[7], M. Gonin[9], A.A. Grigorian[12], S. Grigorian[12], J.Y. Grossiord[11], F.F. Guber[7], A. Guichard[11], H. Gulkanyan[12], R. Hakobyan[12], R. Haroutunian[11], M. Idzik[10,e], D. Jouan[8], T.L. Karavitcheva[7], L. Kluberg[9], A.B. Kurepin[7], Y. Le Bornec[8], C. Lourenço[5], P. Macciotta[4], M. Mac Cormick[8], A. Marzari-Chiesa[10], M. Masera[10], A. Masoni[4], M. Monteno[10], A. Musso[10], P. Petiau[9], A. Piccotti[10], J.R. Pizzi[11], W. Prado da Silva[10,f], F. Prino[10], G. Puddu[4], C. Quintans[6], S. Ramos[6,b], L. Ramello[10,d], P. Rato Mendes[6], L. Riccati[10], A. Romana[9], H. Santos[6], P. Saturnini[2], E. Scalas[10,d], E. Scomparin[10], S. Serci[4], R. Shahoyan[6,g], F. Sigaudo[10], S. Silva[6], M. Sitta[10,d], P. Sonderegger[5,b], X. Tarrago[8], N.S. Topilskaya[7], G.L. Usai[4], E. Vercellin[10], L. Villatte[8], N. Willis[8]

[1] LAPP, CNRS-IN2P3, Annecy-le-Vieux, France.
[2] LPC, Univ. Blaise Pascal and CNRS-IN2P3, Aubière, France.
[3] IFA, Bucharest, Romania.
[4] Università di Cagliari/INFN, Cagliari, Italy.
[5] CERN, Geneva, Switzerland.
[6] LIP, Lisbon, Portugal.
[7] INR, Moscow, Russia.
[8] IPN, Univ. de Paris-Sud and CNRS-IN2P3, Orsay, France.
[9] LPNHE, Ecole Polytechnique and CNRS-IN2P3, Palaiseau, France.
[10] Università di Torino/INFN, Torino, Italy.
[11] IPN, Univ. Claude Bernard Lyon-I and CNRS-IN2P3, Villeurbanne, France.
[12] YerPhI, Yerevan, Armenia.

a) also at UCEH, Universidade de Algarve, Faro, Portugal
b) also at IST, Universidade Técnica de Lisboa, Lisbon, Portugal
c) on leave of absence from York College CUNY
d) Universitá del Piemonte Orientale, Alessandria and INFN-Torino, Italy.
e) also at Faculty of Physics and Nuclear Techniques, Academy of Mining and Metallurgy, Cracow, Poland
f) now at UERJ, Rio de Janeiro, Brazil
g) on leave of absence of YerPhI, Yerevan, Armenia

Abstract

Drell-Yan, J/ψ and ψ' production in proton-induced collisions on Be, Al, Cu, Ag and W targets has been studied by the NA50 collaboration at the CERN SPS. The results are needed to fully understand nuclear suppression of the charmonia states and to provide a solid and accurate reference for the study of the anomalous J/ψ suppression, observed by NA50 in Pb-Pb collisions. We show that J/ψ suppression in proton-nucleus and in Sulfur-Uranium collisions can be understood in terms of nuclear absorption and there is no indication of an additional mechanism in S-U compared to p-A collisions.

1 Introduction

One of the most interesting signatures of QGP formation is J/ψ suppression. In 1996, Matsui and Satz predicted that in a QGP the colour binding potential between the c and $\overline{c}$ quarks would be screened, leading to a measurable reduction of the J/ψ yield [1]. Of course, dissociation processes at the hadronic level can also give a sizeable J/ψ suppression, making somewhat more complicated the interpretation of the experimental results. The NA50 experiment has shown that, while the data from p-p to central S-U collisions can be reasonably explained in terms of J/ψ suppression due to hadronic processes, in Pb-Pb collisions there is an extra suppression ("anomalous suppression") that can not be explained with conventional mechanisms and appear to be due to QGP formation [2], [3], [4], [5]. This conclusion was mainly based of the different behaviour between the J/ψ suppression pattern observed in S-U collisions and the one measured in Pb-Pb interactions. In fact, data on p-A collisions were up to now much less accurate.

The study of J/ψ production in proton-nucleus collisions allows to investigate the absorption mechanisms of the $c\overline{c}$ state in its path across the nucleus. A comparison of p-A data with nucleus-nucleus data helps in disentangling the different sources of hadronic absorption: the nuclear absorption that is present in all nuclear collisions and the interaction of the J/ψ with the other generated secondary particles (comovers). The size of this second effect is up to now poorly known, mainly because of the uncertainty in the theoretical calculation of the J/ψ-hadron cross section.

2 The CERN NA50 experiment and the data taking conditions

The NA50 experiment studies the production of muon pairs in collisions of high intensity relativistic proton or ion beams with various fixed targets. These events come from various sources: the decay of pions and kaons, the decay of hadronic resonances (ϕ, ρ, ω, J/ψ, ψ'), the decay of charmed mesons and the hard scattering processes.

The heart of the NA50 experiment is the NA10 muon spectrometer. A schematic view of the NA50 muon spectrometer is shown in Figure 1.

The muon spectrometer detects dimuons in the rapidity region $3 < y < 4$ and with a polar angle between -60° and 60° in the Collins-Soper reference frame. The transverse momentum acceptance for the J/ψ is nearly flat up to ≈ 4 GeV. A detailed description of the NA50 spectrometer can be found in [6], [7], [8], [9] and [10].

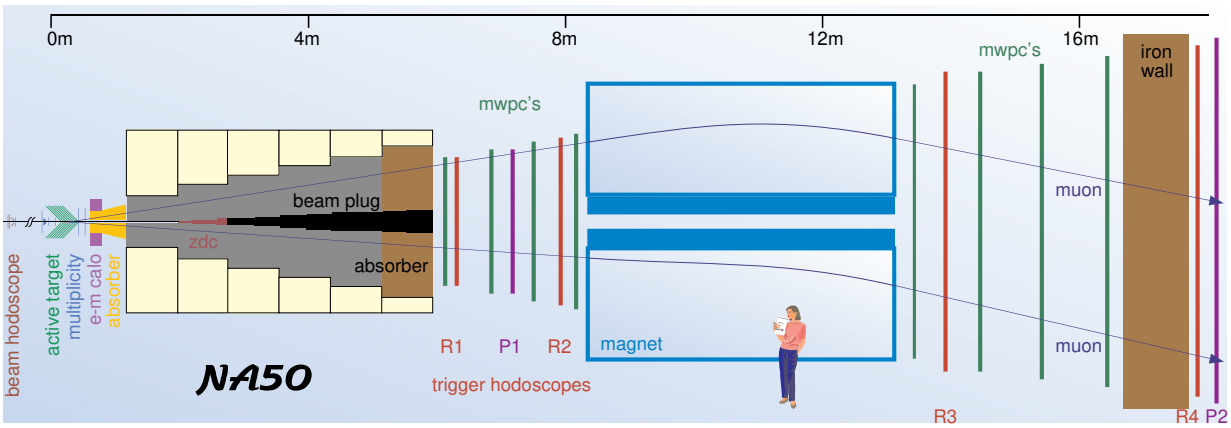

Fig. 1: The NA50 muon spectrometer

Proton-nucleus data have been collected with primary proton beams from the CERN SPS at the energy of 450 GeV. The beam intensity has been chosen around $2 \cdot 10^8$ protons/s to avoid event pile-up in the spectrometer that could spoil the reconstruction efficiency. Consequently the trigger rate is very low (of the order of 20 Hz) and there is practically no dead time.

Five nuclear targets have been used: Be, Al, Cu, Ag and W with thicknesses ranging from 24 g/cm^2 (Be) to 96 g/cm^2 (W).

The sign of the magnetic field has been periodically changed in order to have nearly half of the statistics collected with one sign and the other half with the opposite. This procedure allows to cancel possible small sextant asymmetries that could bias the subtraction of the combinatorial background.

3 Data analysis

Data have been analysed with the traditional procedure. A detailed description of the process can be found in [11]. A kinematical selection of the reconstructed tracks is performed in order to eliminate acceptance edges: $-0.4 < y_{cm} < 0.6$ and $-0.5 < \cos\theta_{CS} < 0.5$.

In Figure 2 the invariant mass spectrum for opposite sign dimuons in the selected kinematic region is presented after cuts. The J/ψ (also ψ) peak is clearly visible. In the same mass region and beyond we have also contribution from the ψ', Drell-Yan (DY) and from the semileptonic decay of charmed hadron pairs ($D\overline{D}$). A contribution due to dimuons from the decay of two pions or kaons (combinatorial background) is also present.

The number of J/ψ, ψ', DY and $D\overline{D}$ events that contribute to the spectrum are estimated by means of a fit. The combinatorial background is estimated from the $\mu^+\mu^+$ and $\mu^-\mu^-$ spectra according to the formula:

$$< N^{+-} >= 2R_{bck} \left\{ \sqrt{(N^{++}N^{--})_{(+)}} + \sqrt{(N^{++}N^{--})_{(-)}} \right\} \quad (1)$$

The factor R_{bck} is necessary to take into account charge correlation effects. It is estimated with a Monte-Carlo simulation based on VENUS 4.12 and ranges from 1.09 to 1.14, depending on target length and beam intensity. A description of the R_{bck} estimation can

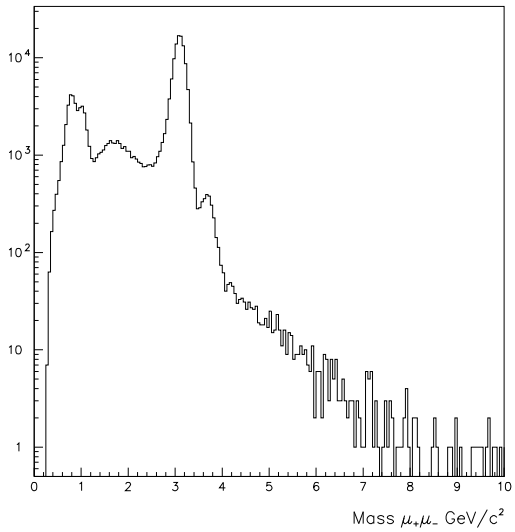

Fig. 2: The invariant mass spectrum for opposite sign dimuons measured in p-Al collisions at 450 GeV/c.

be found in [12] and [13]. The target-out contribution has been estimated with dedicated empty target data taking.

A fit is performed in the region $M_{\mu\mu} > 2\,GeV/c^2$. In Figure 3 the fit to the spectra corresponding to the lightest and heaviest targets are shown. In Figure 4 the contribution of each bin to the global χ^2 is studied showing the good quality of the fit all over the mass range. In particular the crucial region between the J/ψ and the ψ' is well reproduced. The integrated χ^2 is shown for the 5 targets and is compared with lines representing 1 unit χ^2 increase per degree of freedom.

The stability of the results versus the starting point of the fit has been verified.

3.1 Cross section calculations

For the calculation of the absolute cross sections only a selected group of runs collected in very stable conditions has been used.

The luminosity is measured by a set of 3 independent argon counters. They were calibrated with low intensity beams and the linearity of the response was checked up to 10^{10} p/s [14]. The estimated uncertainty on the absolute calibration of the counter response is $\approx 4\%$ and is common to all the measurements. Relative oscillations of the counter response (of the order of 3%) have been observed between the periods of data taking. This has been included in the estimation of the systematic error.

The reconstruction efficiency is larger than 0.97 for all data sets and has an estimated uncertainty of about 1%.

The trigger efficiency has been measured with special runs with dedicated hardware. It ranges from 0.86 to 0.90 with an uncertainty of about 2%. Short range fluctuations of the trigger efficiency have been observed. Their size is lower than 3% and have been included in the estimation of the systematic error.

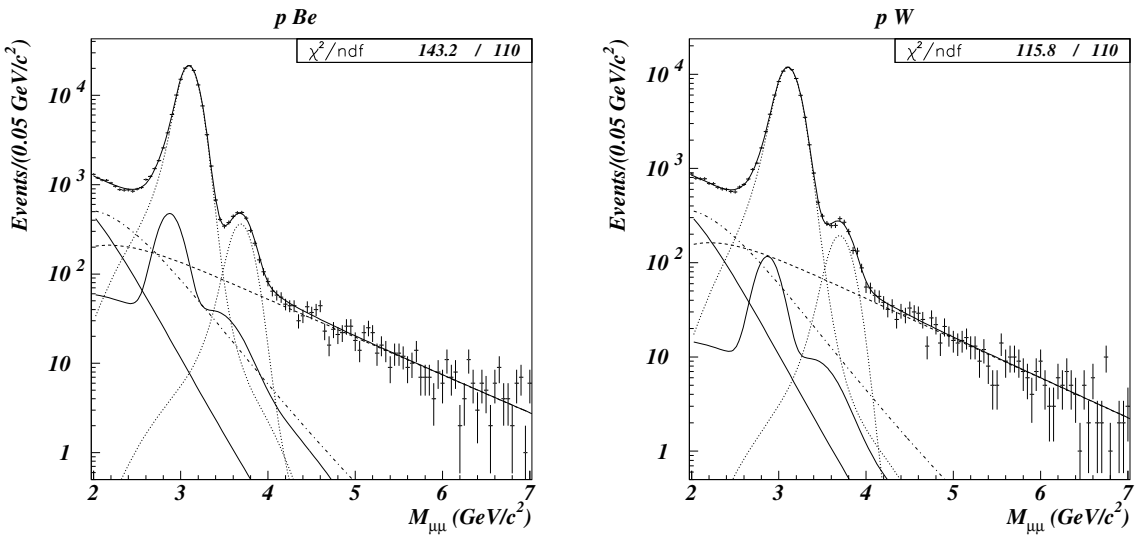

Fig. 3: Fit on the p Be and p W. The upper continuous line is the sum of all the signal contributions: J/ψ and ψ' resonances (dotted lines), the DY continuum (dashed line), the open charm continuum (dashed-dotted line), the background and empty target contributions (continuous lines).

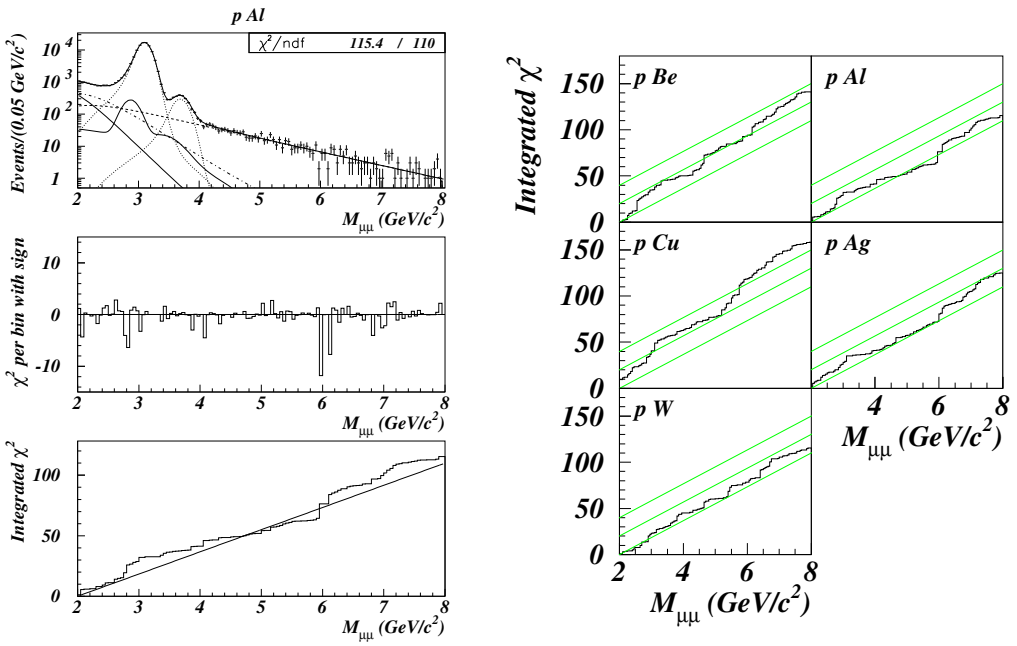

Fig. 4: Fit on the p Al data: (left) the histogram is shown together with the contribution to the fit χ^2 for each bin used in the fit: negative (positive) values means less (more) data than estimated from the fit. The integrated χ^2 in the same region is shown for the p Al data and for the five targets (right). The continuous lines represent for 1 unit χ^2 gain per degree of freedom.

In Figure 5 the J/ψ and ψ' cross sections per target nucleon, measured in the kinematical domain $-0.4 < y_{cm} < 0.6$ and $-0.5 < \cos\theta_{CS} < 0.5$, are plotted against the target mass number together with the results published by NA51 for p-p and p-d interactions [15].

The measured cross sections have been fitted with the function: $\sigma_{p-A} = \sigma_{p-p} * A^{\alpha}$, where A is the mass number of the target. The value of α parametrises nuclear effects. If $\alpha = 1$, this means that the considered hard process does not suffer shadowing (anti-shadowing) effect in the initial state or absorption in the final state. The NA51 points are not included in the fit as this parametrisation is not meaningful for the lightest nuclear targets [16].

For the J/ψ we get $\alpha_{J/\psi} = 0.925 \pm 0.018\,(0.002)$. Concerning errors, the first number represents the total error (statistical + systematic). The number indicated in brackets represents the statistical error only. The a $\chi^2/d.o.f.$ of the fit to J/ψ cross section data is 0.75. For the ψ' is obtained $\alpha_{\psi'} = 0.913 \pm 0.024\,(0.015)$ with a $\chi^2/d.o.f. = 1.0$. The corresponding $\sigma_{J/\psi,\,\psi'}$ are 5.8 ± 0.4 nb/nucleon (J/ψ) and 0.10 ± 0.01 nb/nucleon (ψ').

The DY differential cross section per target nucleon, integrated between 2.9 and 4.5 GeV/c^2 and relative to the same rapidity and $\cos\theta_{cs}$ domain used for J/ψ analysis, is plotted in Figure 6. The isospin dependence of DY production has been corrected using MRS (A) low Q^2 $\overline{MS}$ structure function. The plotted cross sections refer to a nucleus made of A protons, i.e. we study the quantity:

$$\sigma_{pA}^{corrected} = \sigma_{pA}^{measured} \cdot \frac{A \cdot \sigma_{pp}^{calculated\,MRS}}{\sigma_{pA}^{calculated\,MRS}} \tag{2}$$

where the DY cross sections have been calculated at leading order.

For the DY we get is obtained $\alpha_{DY} = 0.993 \pm 0.025\,(0.016)$ and $\sigma_{DY} = 0.093 \pm 0.020$ nb/nucleon, with a $\chi^2/d.o.f. = 0.6$. This shows that nuclear effects (shadowing) are negligible in the explored phase space range, confirming theory predictions given in [17]. Therefore DY can be safely used as a reference process for the study of charmonia production in our kinematical window.

3.2 Ratios of cross sections

When ratios of cross sections are considered, most of the systematic errors cancel. All the uncertainties connected with the normalisation (luminosities, efficiencies) are cancelled by the ratio. The errors on the acceptance calculation do not cancel but are reduced since ratios of acceptances are very stable.

The comparison of resonance cross sections with DY is useful because DY production is proportional to the number of nucleon-nucleon collisions. Therefore the ratio $(J/\psi)/DY$ is proportional to the cross section per nucleon-nucleon collision exactly as $\sigma_{J/\psi}/A$. The drawback of the method is the introduction of larger statistical errors because of the small DY statistics.

In Figure 7 we plot the ratio $B_{\mu\mu}\,\sigma_{J/\psi}/\sigma_{DY}$, where the DY cross section has been integrated over the mass range 2.9-4.5 GeV. The nuclear dependence is extracted with a fit to the five NA50 points studied in this work. As for the absolute cross sections plot the NA51 points are shown but not included in the fit.

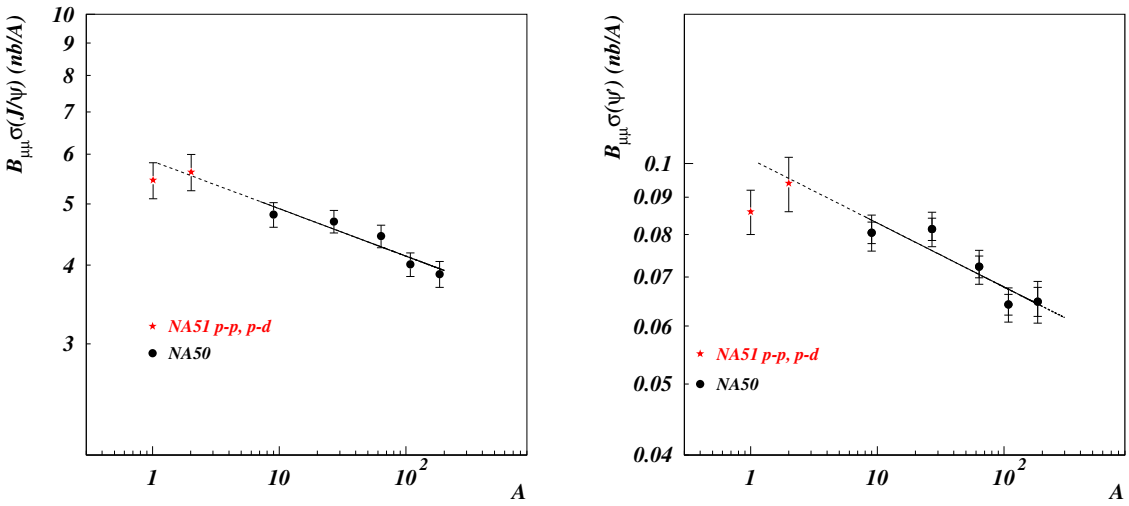

Fig. 5: The J/ψ cross section (left) and the ψ' cross section (right) as a function of the mass number of the target. For the NA50 points (closed circles) the small error bars indicate the statistical uncertainty and the external error bars represent the global (statistical+systematic) uncertainty. For the J/ψ cross sections the statistical error bars are smaller than the symbol size. The result of the fit is shown. The NA51 points are not included in the fit.

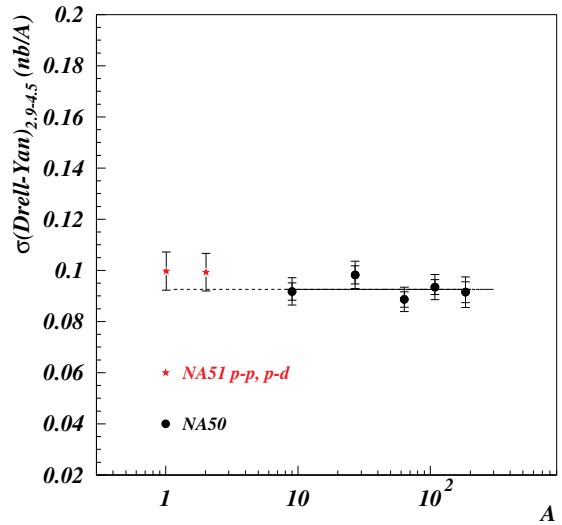

Fig. 6: DY cross section as a function of the mass number of the target. A fit to the NA50 points to extract the α parameter is shown. The NA51 points (p-p and p-d) are shown but not included in the fit. See Figure 5 for description.

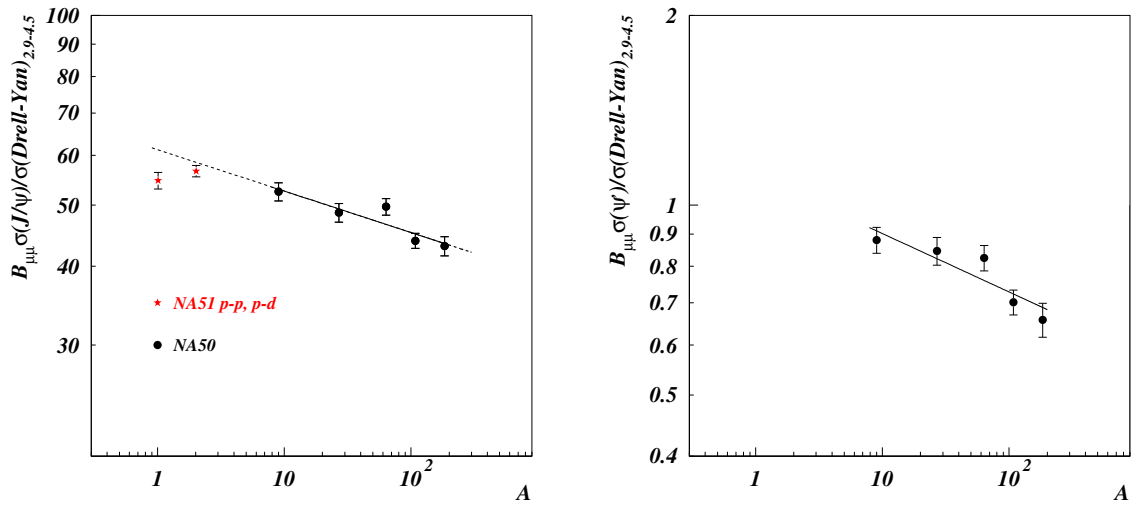

Fig. 7: The ψ/DY and ψ'/DY ratios. A fit to the NA50 points to extract the α parameter is shown. The NA51 points (p-p and p-d) are shown but not included in the fit.

The extracted α values are $\alpha_{J/\psi} = 0.934 \pm 0.014$ with $\chi^2/d.o.f. = 1.7$ and $\alpha_{\psi'} = 0.907 \pm 0.020$ with $\chi^2/d.o.f. = 1.6$.

As for absolute cross sections data indicate a slightly larger nuclear absorption for the ψ' compared to the J/ψ. This appear also in the direct study of $\psi'/(J/\psi)$ ratio, shown in Figure 8. A fit to these points gives: $\Delta\alpha = \alpha_{J/\psi} - \alpha_{\psi'} = 0.029 \pm 0.014\,\text{stat.} \pm 0.003\,\text{syst.}$ with $\chi^2/d.o.f. = 1.1$. If $\Delta\alpha = 0$ is imposed one obtains $B_{\psi'\to\mu\mu}\sigma_{\psi'}/B_{J/\psi\to\mu\mu}\sigma_{J/\psi} = 0.0164 \pm 0.0002$ with a worse $\chi^2/d.o.f. = 1.8$.

4 Comparison with nucleus-nucleus data

The DY process has been used as a reference in the studies of nucleus-nucleus collisions performed by the NA50 collaboration. It has already been shown that in proton-nucleus collisions, the DY is a good reference for J/ψ production since $\alpha = 1$. This is still true when including nucleus-nucleus results [2] so that in comparing p-A and A-A data we can safely use the $(J/\psi)/DY$ ratios.

The comparison has been usually carried out using as independent variable L, the mean length of nuclear matter seen by the pre-resonant $c\overline{c}$ state that will form the J/ψ state [18]. In this framework it is then convenient to study the J/ψ cross section as a function of the length of nuclear matter that the pre-resonant $c\overline{c}$ state has to cross to escape the region where it was produced. In this framework the J/ψ cross section can be written at first order as:

$$\sigma(AB \to J/\psi + X) \propto AB\, exp(-\rho_0 \sigma_{abs} \overline{L}) \tag{3}$$

where: A (B) is the atomic mass of the target (projectile). ρ_0 is the average nuclear matter density: $0.17\,\text{GeV/fm}^3$ and σ_{abs} is an effective cross section for the interaction of

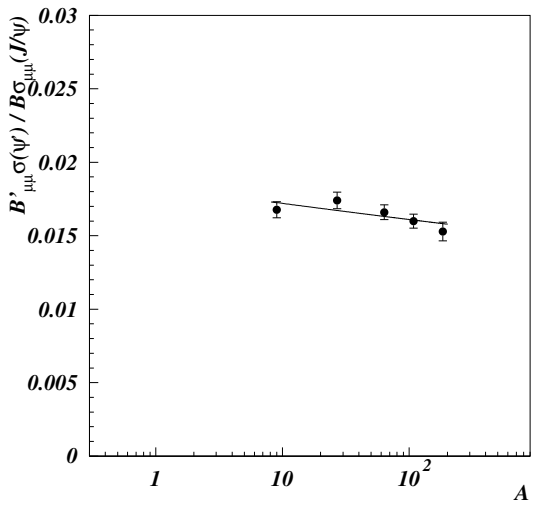

Fig. 8: The ψ'/ψ ratio versus target mass number A. The result of the A^α fit is also shown.

the pre-resonant J/ψ state with nucleons:

$$(J/\psi)_{pre-resonant} + N \rightarrow D\overline{D} + X \tag{4}$$

In Figure 9 we plot the ratios ψ/DY and ψ'/DY versus $\overline{L}$ for the p-A collisions studied in this work and the published results of the NA38 collaboration for S-U collisions at 200 GeV/nucleon [19]. From a simple exponential fit we get the effective cross sections $\sigma^{pA}_{J/\psi\,N} = (4.3 \pm 0.9)$ mb. From a separate fit to the S-U point we get $\sigma^{SU}_{J/\psi\,N} = (5.7 \pm 1.9)$ mb. The difference between the two cross section is $\Delta\sigma^{SU-pA}_{J/\psi\,N} = \sigma^{SU}_{J/\psi\,N} - \sigma^{pA}_{J/\psi\,N} = (1.4 \pm 2.1)$ mb that is compatible with zero. The two data sets can therefore be fitted simultaneously with a common slope: the results $\sigma^{pA}_{J/\psi\,N} = (4.5 \pm 0.8)$ mb with a $\chi^2/d.o.f. = 0.7$.

Clearly this is not possible for the ψ'. From the p-A points at 450 GeV we extract an absorption cross section $\sigma^{pA}_{\psi'\,N} = 6.3 \pm 1.3$ mb. The NA38 collaboration, from a fit to the S-U points found $\sigma^{SU}_{\psi'\,N} = 24 \pm 5$ mb.

To gain a better understanding of J/ψ suppression in p-A and S-U collisions one should correct J/ψ production data for the contributions of the decay of other charmonia resonances. In fact a considerable fraction of the observed J/ψ yield comes from the decay of the χ_c and of the ψ'. While the nuclear dependence of χ_c production is unknown, we have measured the ψ' yield and we can remove its contribution to J/ψ production.

In Figure 10 we plot the measured the ψ/DY data together with the same data corrected for the ψ' contamination. We see that the ψ' feed has the effect to artificially increase the slope difference between p-A and S-U. In fact, after removing these events, the two slopes are more similar ($\Delta\sigma^{SU-pA}_{\psi N} = (0.9 \pm 2.2)$ mb) and the simultaneous fit has a better quality: $\chi^2/d.o.f. = 0.55$.

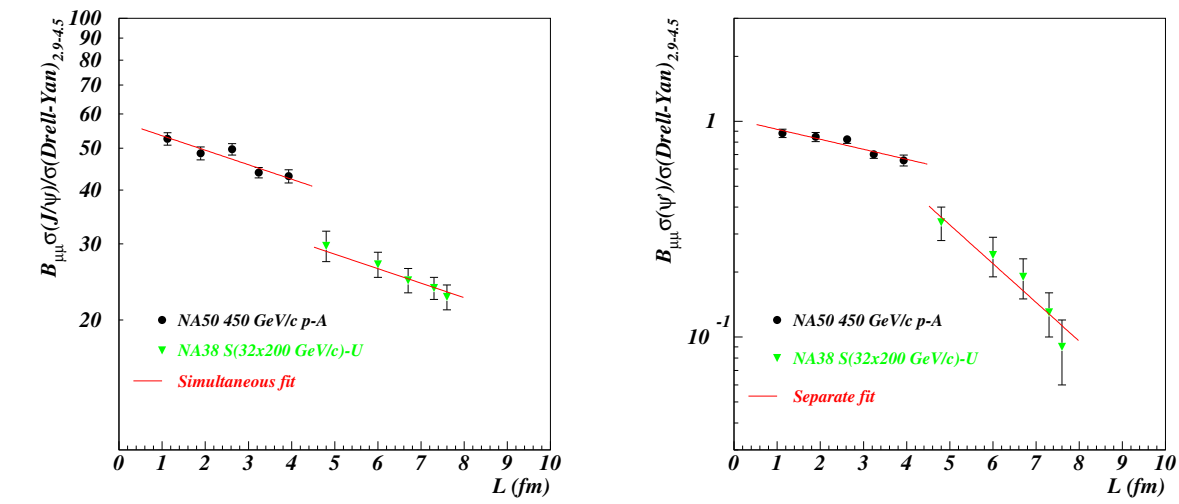

a) b)

Fig. 9: a) The ψ/DY ratio plotted as a function of L. The simultaneous fit to the p-A and S-U points is shown. b) The ψ'/DY ratio, plotted as a function of L. The lines represent two separate fits to p-A and S-U data respectively.

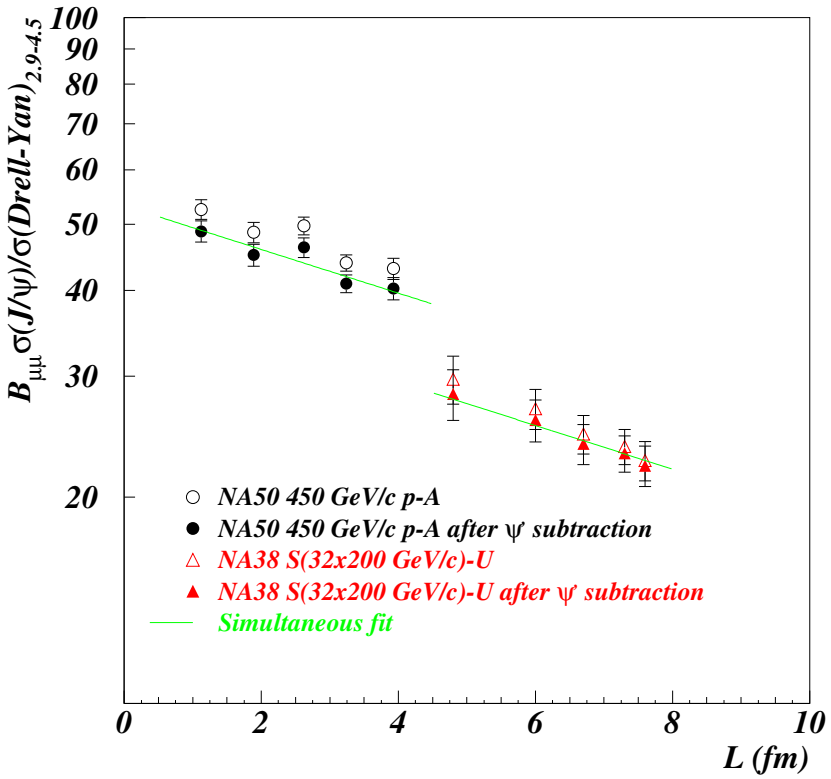

Fig. 10: The ψ/DY ratio in p-A and S-U collisions, before and after the subtraction of J/ψ contamination from the ψ' decay.

5 Conclusions

Cross sections and ratios of cross sections for charmonia and Drell-Yan production in p-A collisions have been measured by NA50 at 450 GeV incident energy in the rapidity region $-0.4 < y_{cm} < 0.6$ on Be, Al, Cu, Ag and W targets.

Fitting the DY cross section data with a power law A^α we get $\alpha_{DY} = 0.993 \pm 0.025$. This value is compatible with unity, confirming the theoretical expectation, that in p-A collisions at 450 GeV, in our kinematical domain, shadowing effects are negligible. Being proportional to A the Drell-Yan can be used as a good reference to study a hard process as charmonium production.

This led us to consider the ratios of charmonia production cross sections with DY, $\sigma_{J/\psi}/\sigma_{DY}$ and $\sigma_{\psi'}/\sigma_{DY}$, which are equivalent to a measurement of the cross sections per nucleon-nucleon collision. Using this ratio one cancels most of the systematic errors. In this way we obtained the following estimation of the nuclear dependence of the charmonia cross sections: $\alpha_{J/\psi} = 0.934 \pm 0.014$ and $\alpha_{\psi'} = 0.907 \pm 0.020$. The charmonia α values deviate significantly from one, indicating a sizeable nuclear absorption.

From the direct analysis of the $\sigma_{J/\psi}/\sigma_{\psi'}$ ratio we extract $\Delta\alpha = \alpha_{J/\psi} - \alpha_{\psi'} = 0.029 \pm 0.014$. This results indicate at a 2σ level that there is a difference between $\sigma_{J/\psi\,N}$ and $\sigma_{\psi'\,N}$ at this energy. This result qualitatively confirms the results of E866 experiment that first measured, at higher energies (800 GeV), a difference between J/ψ and ψ' behaviour [20].

The NA50 p-A data have been then compared with NA38 S-U data , where charmonia absorption by hadronic comovers is in principle possible.

Concerning ψ', an extrapolation of p-A points completely fails in reproducing the observed S-U results. The much steeper slope of ψ'/DY versus $\overline{L}$ in S-U indicates the presence of a further absorption mechanism, namely comovers absorption.

For what concerns the J/ψ the slopes appear to be compatible and the two data sets can be fitted with a common nuclear absorption cross section, corresponding in the simple exponential fit approximation to $\sigma^{pA}_{J/\psi\,N} = (4.5 \pm 0.8)$ mb.

When the feed to J/ψ yield coming from the decay of ψ' is subtracted the slope of the S-U points considerably flattens leading to an even better compatibility between p-A and S-U. Therefore no additional source of J/ψ suppression has to be introduced to explain S-U data compared to p-A.

References

[1] T. Matsui and H. Satz, Phys. Lett. B 178 (1986) 416.

[2] M.C. Abreu et al., Ph. Lett. B 410 (1997) 337.

[3] M.C. Abreu et al., Ph. Lett. B 450 (1999) 456.

[4] M.C. Abreu et al., Ph. Lett. B 477 (2000) 28.

[5] R. Arnaldi, Ph.D. thesis, 2000, Clermont.

[6] M.C. Abreu et al., Phys. Lett. B 410 (1997) 327.

[7] R. Arnaldi et al., Nucl. Instr. and Meth. A 409 (1998) 608.

[8] R. Arnaldi et al., Nucl. Instr. and Meth. A 409 (1998) 608.

[9] S. Beolé, Ph.D. thesis, 1998, Torino.

[10] F. Bellaiche et al., Nucl. Instr. and Meth. A 398 (1997) 180.

[11] P. Cortese, Ph.D. thesis, 2000, Torino.

[12] C. Soave, Ph.D. thesis, 1998, Torino.

[13] M.C. Abreu et al., Eur. Phys J. C 14 (2000) 443.

[14] L. Fredj, Ph.D. thesis, 1991, Clermont.

[15] M.C. Abreu et al., Phys. Lett. B 438 (1998) 35.

[16] R. Vogt, Phys. Rep. 310 (1999) 197.

[17] K.J. Eskola et al., JYFL-4/00 (Sep. 2000).

[18] C. Gerschel and J. Hufner, Z. Phys. C 56, (1992) 171.

[19] M.C. Abreu et al., Phys. Lett. B 466 (1999) 408.

[20] M.J. Leitch et al., Phys. Rev. Lett. 84, 3256-3260 (2000).